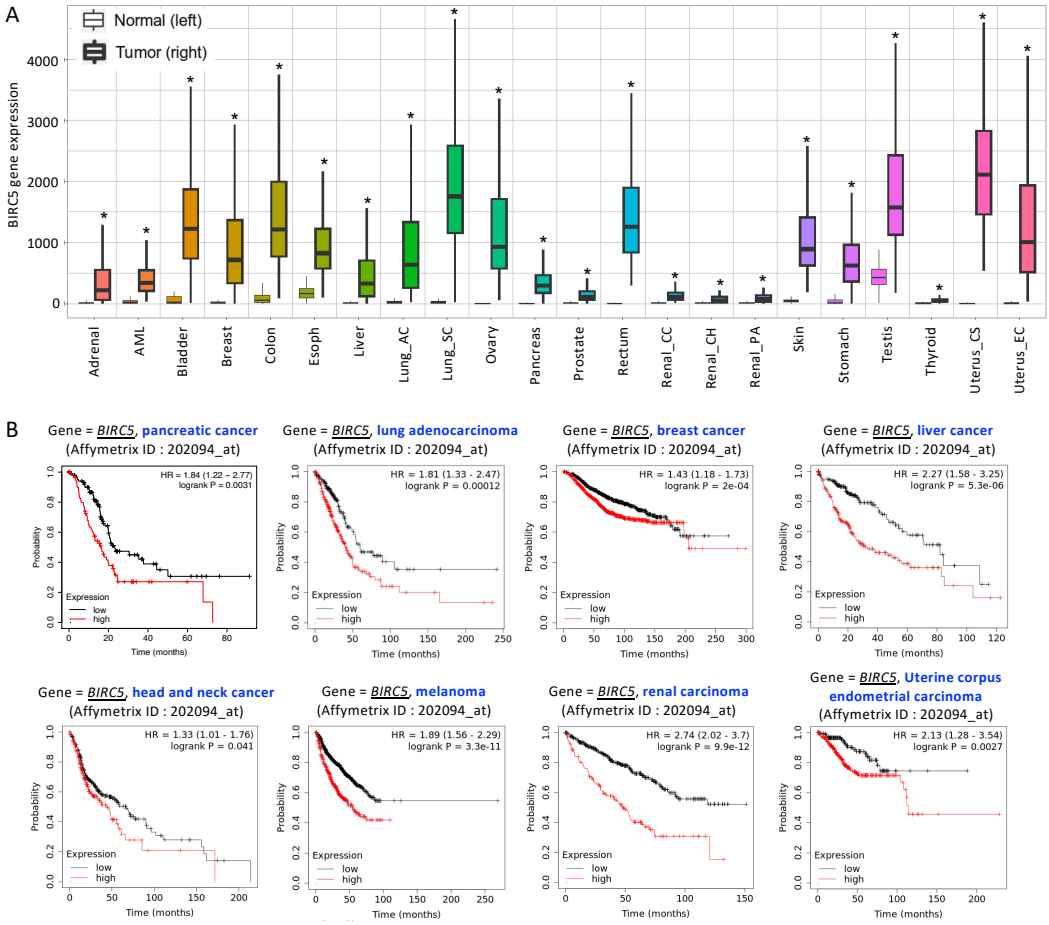

Figure S1 – BIRC5 is overexpressed in tumor tissues across multiple cancer types, and elevated BIRC5 expression correlates with poor overall survival in cancer patients. (**A**) Bar graph depicting mRNA expression levels of BIRC5 in various normal tissues (left, thin border) compared to tumor tissues (right, thick border). Expression data were obtained from GEO, TCGA, GTEx, and TARGET databases and analyzed using the TNM Plotter online tool. (**B**) Kaplan-Meier overall survival curves for cancer patients with high (*BIRC5*^{high}, red curve) versus low (*BIRC5*^{low}, black curve) *BIRC5* expression, including pancreatic, lung, breast, liver, head and neck, melanoma, renal carcinoma, and uterine corpus endometrial cancers. Survival analysis was performed using the Kaplan-Meier plotter online database (https://kmplot.com/).*$P < 0.05$ *vs.*

normal tissues

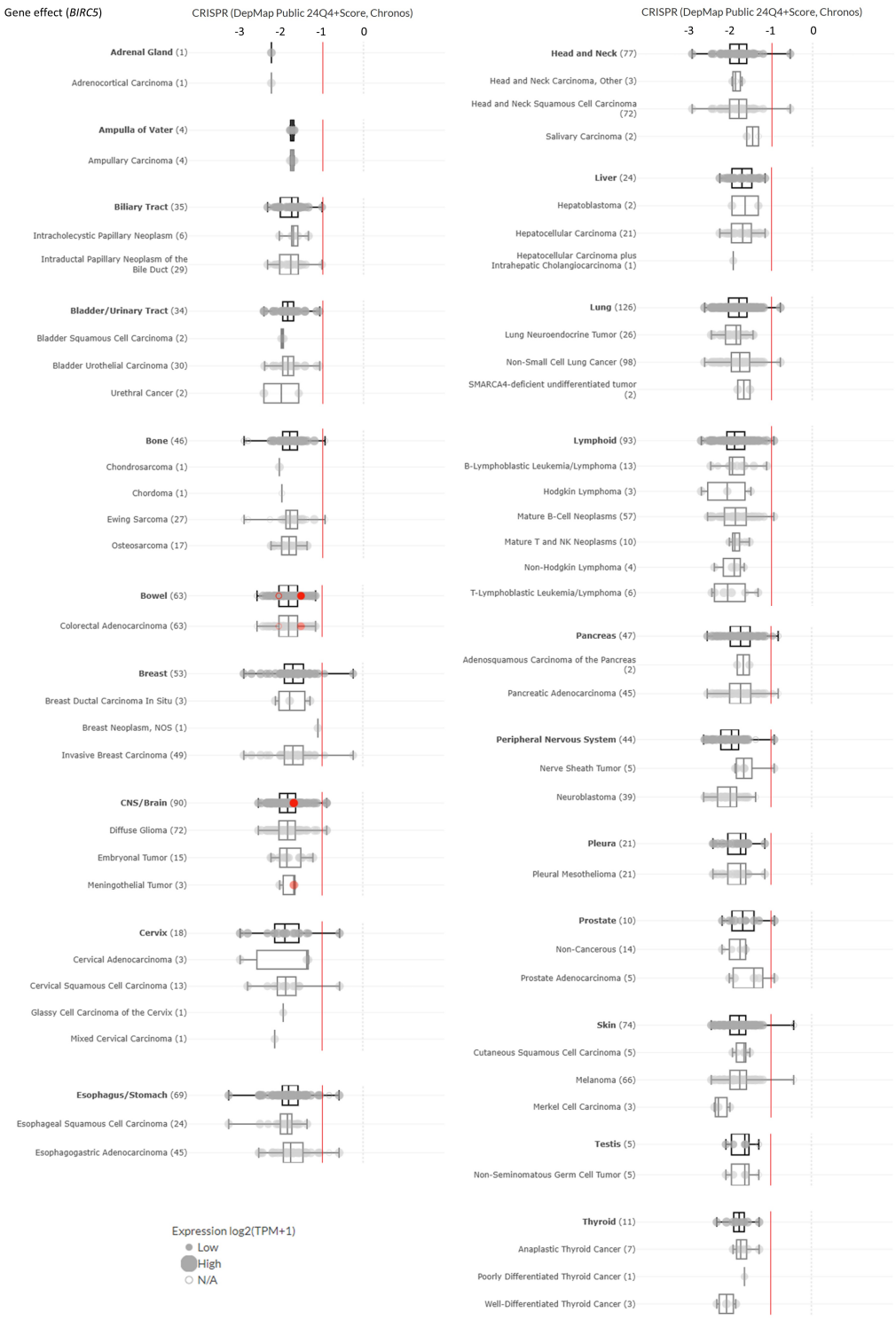

Figure S2 – Association of *BIRC5* with survival dependency across various cancer cell types. Graph illustrating the expression levels and gene dependency effects of *BIRC5* in multiple cancer cell lines, generated using data from the DepMap portal (https://depmap.org/portal/). Gene dependency is represented by the Chronos

dependency score, where lower scores indicate a higher likelihood that *BIRC5* is essential for cell survival. A score of 0 signifies a non-essential gene, while a score of –1 corresponds to the median dependency of all pan-essential genes (indicated by the red line).

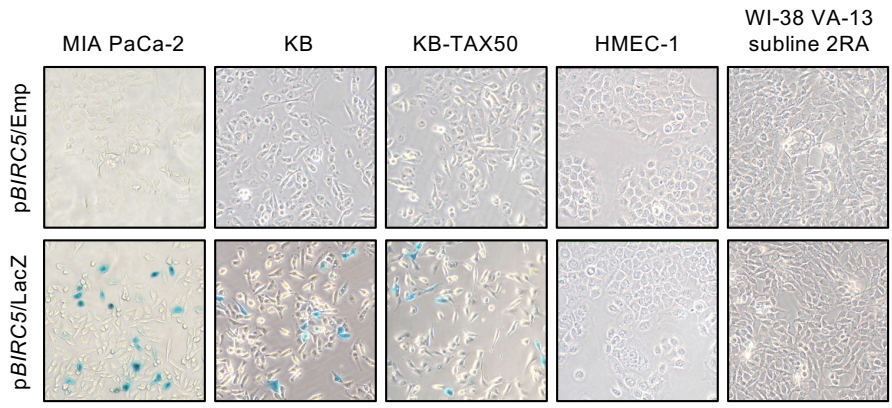

Figure S3 – *BIRC5* promoter activity in cancer and normal cell lines. MIA PaCa-2, KB, KB-TAX50, HMEC-1, and WI-38 VA-13 subline 2RA cells were transfected with p*BIRC5*/Emp and p*BIRC5*/LacZ for 24 h. The *BIRC5* promoter activity was analyzed with the β-galactosidase staining.

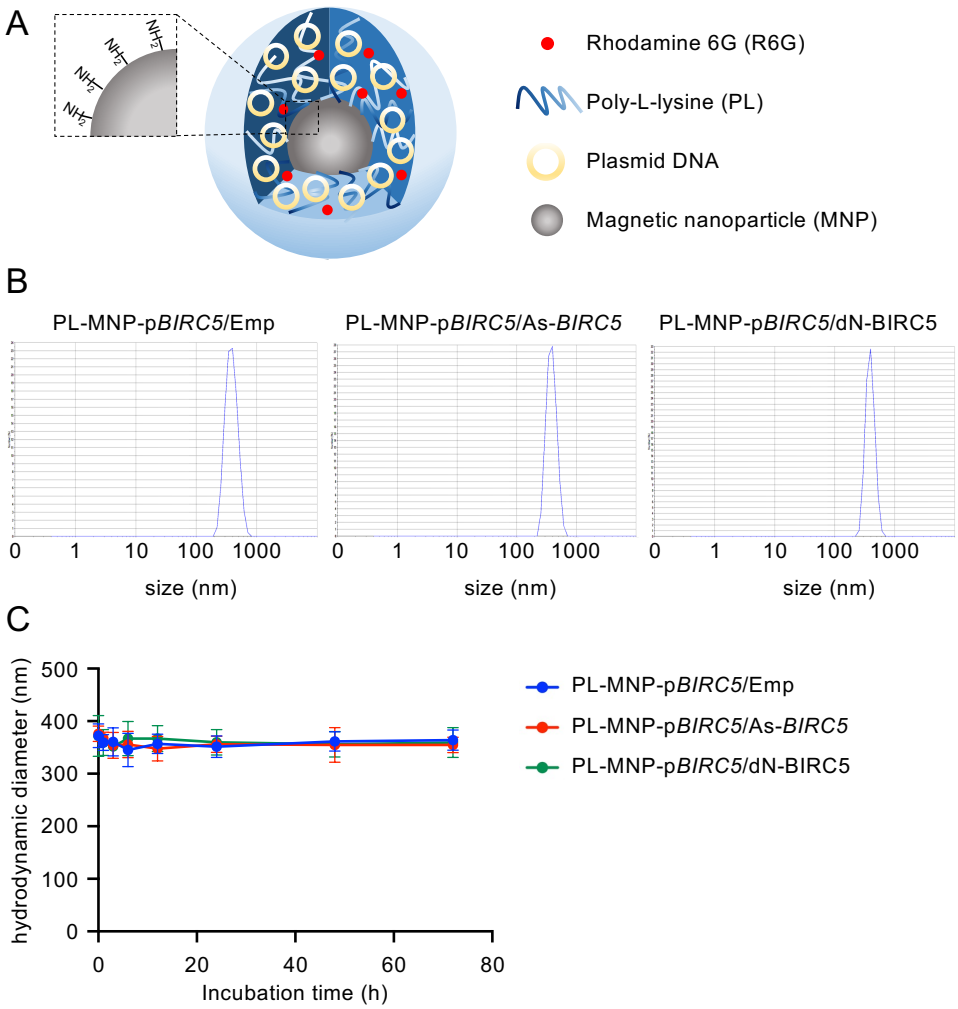

Figure S4 – Physicochemical characterization and serum stability of PL-MNP. (**A**) Schematic diagram illustrating the structure of poly-L-lysine-modified plasmid DNA-adsorbed magnetic nanoparticles (PL-MNPs). (**B**) Hydrodynamic diameters of PL-MNP-p*BIRC5*/Emp, PL-MNP-p*BIRC5*/As-*BIRC5*, and PL-MNP-p*BIRC5*/dN-BIRC5 measured by DLS. (**C**) PL-MNP-p*BIRC5*/Emp, PL-MNP-p*BIRC5*/As-*BIRC5*, and PL-MNP-p*BIRC5*/dN-BIRC5 were incubated in RPMI medium (10% FBS and 1% PSG) for the indicated times. DLS measured the hydrodynamic diameters. Data represent at least three independent experiments. The statistical analysis was performed using one-way ANOVA (P>0.05).

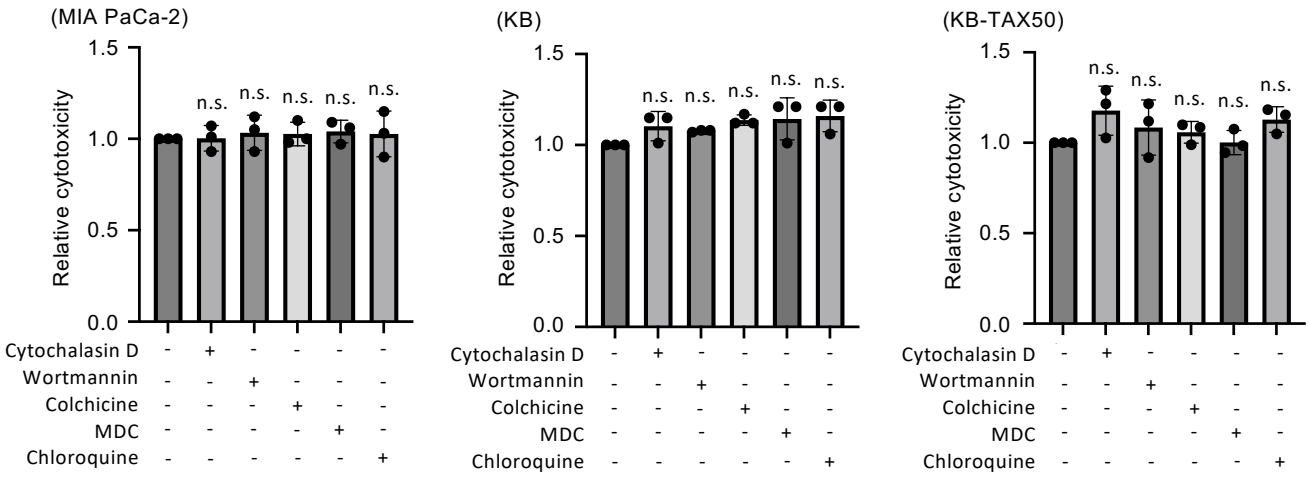

Figure S5 – The cell cytotoxicity of the endocytosis inhibitors in cancer cell lines.

MIA PaCa-2, KB, and KB-TAX50 cells were treated with endocytosis inhibitors, including 10 μM cytochalasin D, 50 nM wortmannin, 10 μM colchicine, 200 μM monodansylcadaverine (MDC), or 125 μM chloroquine, for 24 h. The cell cytotoxicity was measured by the Cytotoxicity LDH assay. Data represent at least three independent experiments. The statistical analysis was performed using one-way ANOVA ($P>0.05$).

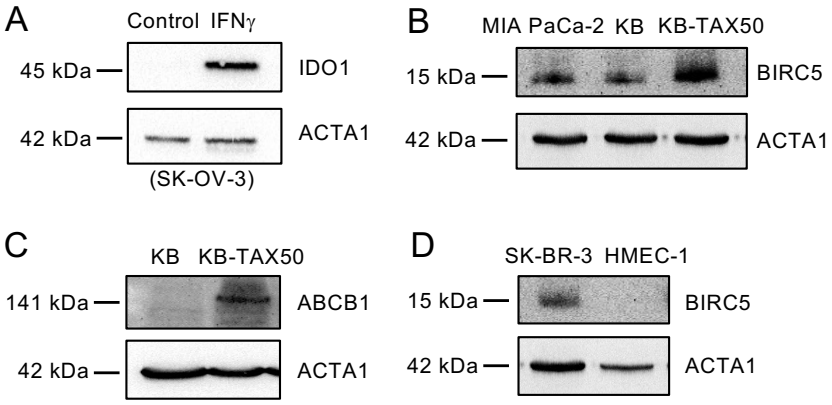

Figure S6 – IDO, BIRC5, and ABCB1 expression in the tested cell lines. (**A**) Western blot analysis of IDO expression in IFNα-treated SK-OV-3 cells. (**B**) Western blot analysis of BIRC5 expression in MIA PaCa-2, KB, and KB-TAX50 cells. **(C)** Western blot analysis of ABCB1 expression in KB and KB-TAX50 cells. (**D**) Western blot analysis of BIRC5 expression in SK-BR-3 and HMEC-1 cells. ACTA1 served as a loading control to verify equal protein loading.

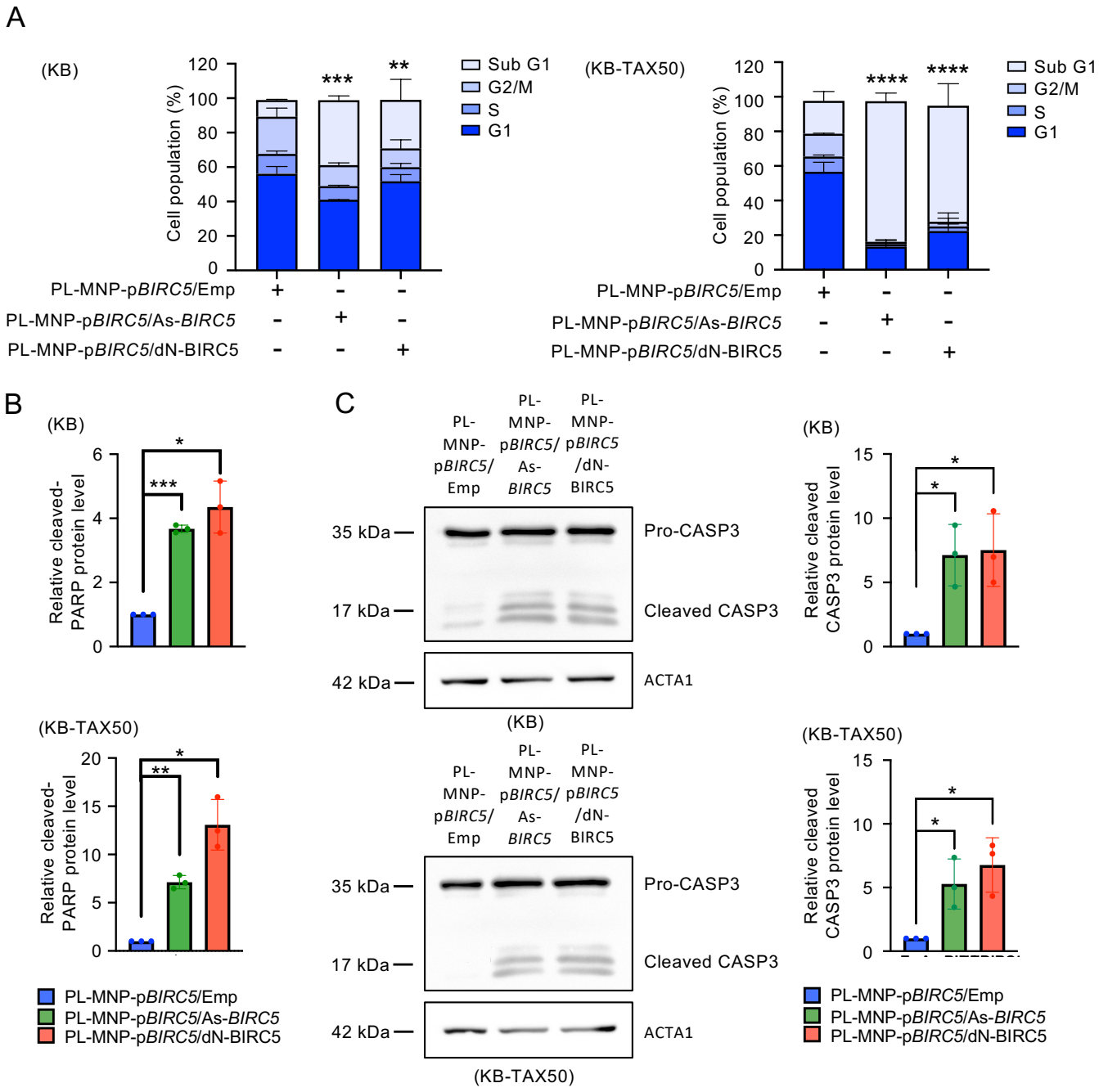

Figure S7 - BIRC5-targeting PL-MNPs demonstrate equal potency against ABCB1-non-expressing and ABCB1-expressing cancer cells. (A) KB and KB-TAX50 cells were treated with PL-MNP-p*BIRC5*/As-*BIRC5* or PL-MNP-p*BIRC5*/dN-BIRC5 at their respective IC_{50} concentrations for 72 h. Following treatment, cells were stained with propidium iodide (PI) and analyzed by flow cytometry. Data represent at

least three independent experiments. (B) The bar graph represents the quantified band intensities from independent experiments, with cleaved-PARP expression levels normalized to the corresponding ACTA1 band intensity for each sample, corresponding to the representative blots shown in Figure 6B. (**C**) CASP3 expression in KB and KB-TAX50 cells treated with PL-MNP-p*BIRC5*/As-*BIRC5* or PL-MNP-p*BIRC5*/dN-BIRC5 for 48 h, determined by Western blotting. ACTA1 served as a loading control. Data represent at least three independent experiments. The bar graphs represent the quantified band intensities from independent experiments, with cleaved CASP3 expression levels normalized to the corresponding ACTA1 band intensity for each sample. All bar graphs indicate the mean ± SD. The statistical analysis was performed using one-way ANOVA. *$P < 0.05$, **$P < 0.01$, ***$P < 0.001$, ****$P < 0.0001$ vs. PL-MNP-p*BIRC5*/Emp.

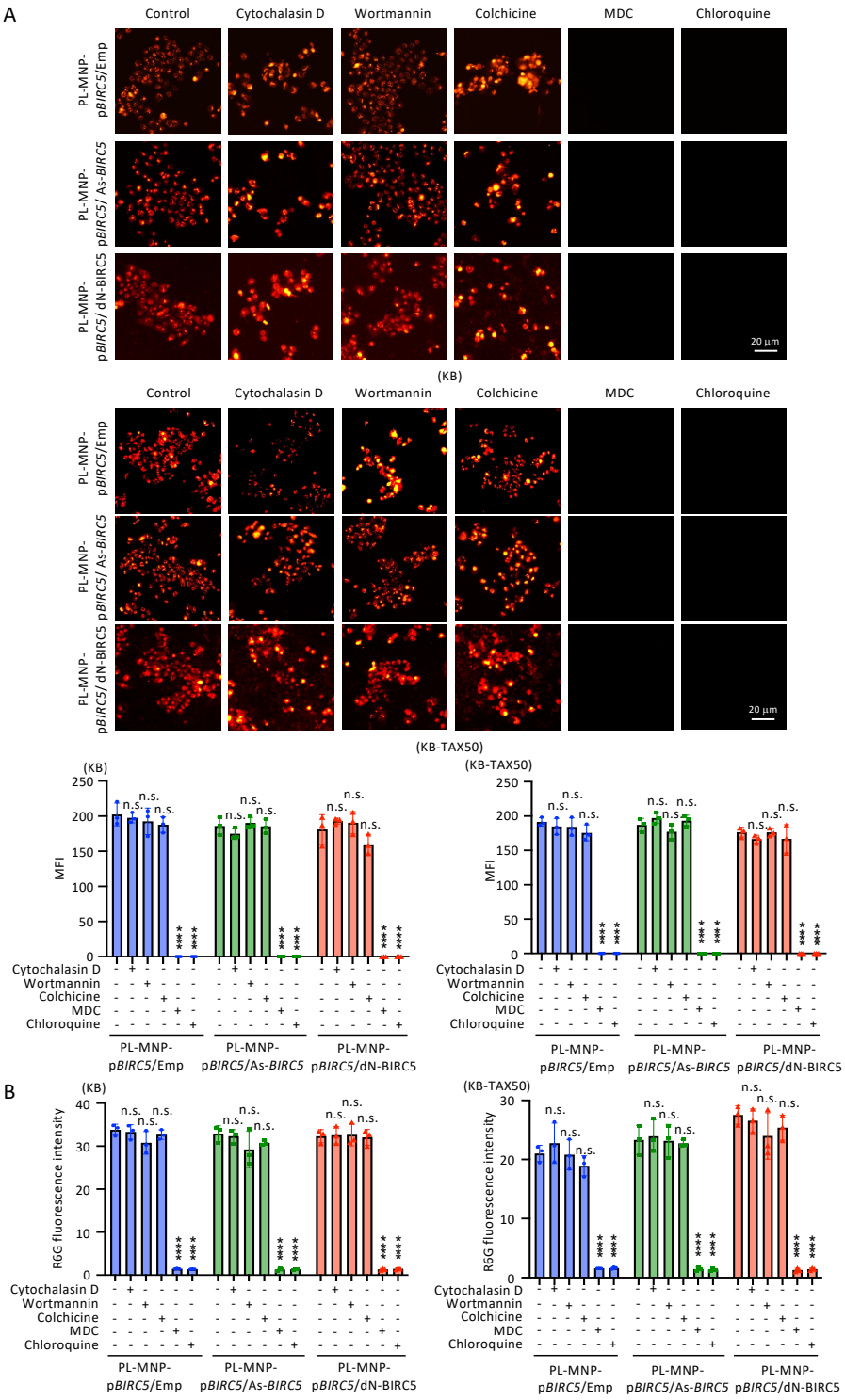

Figure S8 – Uptake of PL-MNP-p*BIRC5*/As-*BIRC5* and PL-MNP-p*BIRC5*/dN-BIRC5 *via* clathrin-mediated endocytosis in KB and KB-TAX50 cells. KB and KB-TAX50 cells were pretreated with endocytosis inhibitors, 10 μM cytochalasin D, 50 nM wortmannin, 10 μM colchicine, 200 μM MDC, and 125 μM chloroquine, for 30 min.

Cells were then incubated with 10 ng/μL PL-MNP-p*BIRC5*/Emp, PL-MNP-p*BIRC5*/As-*BIRC5*, or PL-MNP-p*BIRC5*/dN-BIRC5 for 24 h. **(A)** Uptake efficiency was assessed by fluorescence microscopy, and the fluorescent intensity was quantified with ImageJ. **(B)** Cells were lysed with Cellytic™ M reagent, and fluorescence intensity was measured using a SpectraMax ID3 microplate reader. Data represent at least three independent experiments. Bar graphs indicate the mean ± SD. The statistical analysis was performed using one-way ANOVA. ****$P < 0.0001$ vs. untreated control (no inhibitor); n.s., not significant.